



124  
348  
THS

THESIS



This is to certify that the  
thesis entitled

Lineshapes in Infrared Laser Stark Spectroscopy

presented by

Scott Sandholm

has been accepted towards fulfillment  
of the requirements for

Masters degree in Chemistry

A handwritten signature in cursive script, reading "R. H. Schwendeman". The signature is written in dark ink and is positioned above the title "Major professor".

Major professor

Date 7 May 1979

MICHIGAN STATE UNIVERSITY LIBRARIES



3 1293 00998 9348

L



MSU

OVERDUE FINES ARE 25¢ PER DAY  
PER ITEM

Return to book drop to remove  
this checkout from your record.

MSU 1924



LINESHAPES IN INFRARED LASER  
STARK SPECTROSCOPY

By

Scott Sandholm

A THESIS

Submitted to

Michigan State University

in partial fulfillment of the requirements  
for the degree of

MASTER OF SCIENCE

Department of Chemistry

1979

## ABSTRACT

### LINESHAPES IN INFRARED LASER STARK SPECTROSCOPY

By

Scott Sandholm

The Doppler-broadened lineshapes of selected transitions in the  $\nu_3$  band of  $\text{CH}_3\text{F}$  have been investigated. The transitions studied are among those that can be brought into resonance with the  $\text{CO}_2$  laser lines near  $1050\text{ cm}^{-1}$  by application of an electric field. The laser Stark spectrometer used in the investigation and the necessary vibration-rotation theory are described. Relative intensities of transitions occurring at different electric fields, but with the same laser line, were found to follow predicted values to approximately 5%. The derivatives of the frequencies of the transitions with respect to electric field have been estimated from linewidths with an average deviation from predicted values of 2.3%. In addition, the relative intensities of a given transition appear to be a linear function of pressure to within a mean deviation of 4.7%. The effect of modulation broadening and sample pressure on the appearance of the lineshape have also been investigated.

To Linda

## ACKNOWLEDGMENT

Special thanks are due Dr. R. H. Schwendeman for the many useful discussions and his moral support through all the difficult hours in the laboratory, as well as in preparing this Thesis. I would also like to thank Dr. Erik Bjarnov for his assistance in the laboratory and especially for the modification of the computer program GDFITB. I am grateful for the numerous helpful discussions with John Leckey and Keith Peterson. Also, financial aid from the National Science Foundation is gratefully acknowledged.

## TABLE OF CONTENTS

Chapter	Page
LIST OF TABLES . . . . .	v
LIST OF FIGURES . . . . .	vii
LIST OF ABBREVIATIONS . . . . .	ix
I. INTRODUCTION . . . . .	1
II. EXPERIMENTAL . . . . .	4
2.1. The Laser . . . . .	4
2.2. The Sample Cell . . . . .	7
2.3. The Laser Stark Spectrometer . . . . .	7
2.4. Computer Programs . . . . .	11
III. THEORY . . . . .	14
3.1. The Stark Effect . . . . .	14
3.2. Lineshapes . . . . .	20
IV. RESULTS AND CONCLUSIONS . . . . .	27
4.1. Introduction . . . . .	27
4.2. The Gaussian Lineshape . . . . .	31
4.3. Modulation Broadening . . . . .	32
4.4. The Effect of Sample Pressure . . . . .	38
4.5. Determination of the Laser Stark Slopes . . . . .	41
4.6. Relative Intensities . . . . .	46
4.7. The Dependence of Absorption on Sample Pressure . . . . .	50
4.8. Discussion . . . . .	50
REFERENCES . . . . .	54

## LIST OF TABLES

Table		Page
I	Laser Stark Transitions in $\text{CH}_3\text{F}$ that were Studied in this Investi- gation. . . . .	28
II	Experimental Resonant Voltages Obtained from Least Squares Fits of Experimental Data to Theoretical Lineshapes and Derived Values of the Cell Spacing. . . . .	29
III	Variation of the Apparent Doppler Width of the $R(1,1)$ , $m=0\leftarrow 1$ Transi- tion with the Voltage Applied to the Piezoelectric Translator. . . . .	36
IV	Variation of the Apparent Doppler Width of the $R(1,0)$ , $m=0\leftarrow 1$ Transi- tion with the Voltage Applied to the Piezoelectric Translator. . . . .	37
V	The Effect of Moderate Pressure Changes on the Apparent Doppler Width for the $R(1,1)$ , $m=0\leftarrow 1$ Transition. . . . .	39
VI	The Effect of Moderate Pressure Variations on the Apparent Doppler Width of the $P(2,1)$ , $m=1\leftarrow 0$ Transition. .	40

Table		Page
VII	Laser Stark Slopes Determined from Experimental Data for the Transitions Investigated. . . . .	44
VIII	Linear Least Squares Parameters for the Relative Intensity Data Depicted Graphically in Figures (6) and (7). . . .	49

## LIST OF FIGURES

Figure		Page
1	A block diagram of the laser Stark spectrometer used in these experiments . . . . .	9
2	A theoretical plot of absorption frequency as a function of electric field for the P(2,1) and P(2,0) transitions in methyl fluoride where $\Delta m = \pm 1$ selection rules are assumed . . . .	18
3	A photograph of an oscilloscope plot of the data file for the R(1,1) $m = -1 \leftarrow 0$ transition in methyl fluoride. . .	33
4	A photograph of an oscilloscope plot of the difference between experimentally observed data and the best theoretical Gaussian line-shape for the R(1,1), $m = -1 \leftarrow 0$ transition in methyl fluoride magnified 140 times . . . . .	34
5	A graph of the square root of the exponential parameter as a function of the scaled Stark slope for determination of the Doppler width. . . .	43

Figure		Page
6	A graph of the signal amplitude (pre-exponential) as a function of theoretical intensity. . . . .	47
7	A graph of the area of a transition as a function of the theoretical intensity . . . . .	48
8	A graph of the relative intensity as a function of pressure for the P(2,1), $m=1 \leftarrow 0$ transition at three different Stark modulation ampli- tudes . . . . .	51

## ABBREVIATIONS

NRC	National Research Council.
PZT	Piezoelectric translator.
$\hat{H}$	Hamiltonian operator.
$\mu_{if}$	Transition dipole moment from state $i$ to state $f$ .
$\mu_F$	The molecular dipole moment component along the F space fixed axis (the direction of the electric field vector).
$\hat{P}$	Total angular momentum operator.
J	Total angular momentum quantum number.
m	Projection of J onto the space fixed Z axis.
k	Projection of J onto the molecule fixed z axis.
P(22)	The P(22) laser line where the transition $J'' \leftarrow J'$ is from $J'=22$ to $J''=21$ .
R(J,k)	Symmetric top transition $J+1 \leftarrow J$ , $k \leftarrow k$ .
P(J,k)	Symmetric top transition $J-1 \leftarrow J$ , $k \leftarrow k$ .
$\omega_s$	Frequency of radiation in the laboratory frame of reference.
$\omega_J$	The Doppler frequency shift.
$k_B$	Boltzmann's constant.
$\Delta\omega_L$	The Lorentzian half-width at half-height.
$\Delta\omega_D$	The Doppler half-width at half-height; i.e., the Doppler width.
$\gamma_0$	Peak absorption coefficient.
$\Gamma$	Integrated or absolute absorption coefficient.
OPS	Operational Power Supply.
K	$ k $ .
M	$ m $ .

## I. INTRODUCTION

Since the mid-1960's laser spectroscopy experiments in the infrared region of the electromagnetic spectrum have been performed in which structural parameters of numerous molecules have been determined.<sup>(1-4)</sup> Laser Stark spectroscopy, one of the laser techniques developed during this time, has become a useful tool for obtaining structural information. In this relatively new form of spectroscopy, the absorption of a sample irradiated by a fixed frequency laser is measured as a function of applied electric field. Rotational constants, dipole moments, centrifugal distortion constants, and Coriolis coupling constants have been obtained by laser Stark experiments.

This thesis describes an investigation to determine whether measurements of the lineshapes of laser Stark transitions would be of assistance in the assignment of the transitions. The difficult process of assignment is the first step in the analysis of a laser Stark spectrum. The basic technique for analyzing the lineshapes of laser Stark transitions is quite simple in principle, but not necessarily so in practice. The intensities of the transitions are recorded as a function of electric field and fit to a Gaussian lineshape by a least squares fitting program. The lineshape is Gaussian as a result of the Doppler effect, which is the main broadening process for gases at

low pressure in the infrared region of the electromagnetic spectrum. By comparing the pre-exponentials (the transition amplitudes) from the least squares fit, it is possible to compare the relative intensities of nonoverlapping transitions that fall on the same laser line, but at different electric fields. At present, relative intensities of transitions on different laser lines are not compared because of the difficulty in obtaining the same output power and optical alignment for the different laser lines. The Stark slopes (change in frequency per change in electric field) of the various transitions are determined from the exponential constants and the theoretical Doppler width. From the slopes, zero field frequencies may be estimated. The relative intensity and the Stark slope data are not obtained in conventional laser Stark experiments. This information along with the electric fields and laser frequencies of the transitions from a conventional laser Stark experiment should help alleviate some of the difficulties in assigning energy levels. This information should also facilitate the calculation of precise rotational constants and dipole moments. It is also possible that the relative intensities and Stark slopes will be useful in applications of laser Stark spectroscopy for chemical analysis.

Methyl fluoride was selected as the initial sample for the lineshape investigation because its spectrum consists of many strong absorption lines that may be observed at

convenient electric fields with easily obtainable CO<sub>2</sub> laser lines. In addition, methyl fluoride had been thoroughly studied by laser Stark techniques at the National Research Council of Canada in 1974 by Freund and associates.<sup>(2)</sup> Several of the transitions assigned by the NRC group were selected for lineshape studies performed in our laboratory.

## II. EXPERIMENTAL

### 2.1. The Laser

The CO<sub>2</sub> laser is a good example of a fixed-frequency laser and is a common source of radiation power for laser experiments in the infrared region. There are several advantages to a fixed-frequency laser compared to a tunable laser.<sup>(3)</sup> Since the laser frequencies have been determined very accurately by beating the laser output against harmonics of lower frequencies, time-consuming calibration procedures and the expense of calibration equipment are not necessary. Also, the fixed frequency CO<sub>2</sub> laser is more monochromatic and has higher power than presently available tunable infrared lasers. The main disadvantage of a fixed frequency laser is the fact that absorption occurs only at those frequencies corresponding to quantum-mechanically allowed transitions. Therefore, absorption of radiation from a fixed frequency laser is obtained only if a fortunate coincidence occurs or if the molecular transition frequencies can be tuned by an electric or magnetic field.

In 1965 Patel discovered that a CO<sub>2</sub> molecular laser would function with a mixture of CO<sub>2</sub> and N<sub>2</sub> gas, where the CO<sub>2</sub> molecules are excited by collisions of the second kind with vibrationally excited N<sub>2</sub> molecules. Since the N<sub>2</sub> molecule has no permanent dipole moment, it cannot relax back to the ground state through electric dipole radiation.

Therefore if  $N_2$  is excited to its  $v=1$  vibrational level in the ground electronic state, it must relax through collisions with the walls or with other molecules. The  $CO_2$  molecule, whose  $00^{\circ}1$  ( $\Sigma_u^+$ ) level is close in energy to the  $v=1$  level of  $N_2$ , becomes the important collision partner. When a population inversion occurs between the  $00^{\circ}1$  level and either the  $10^{\circ}0$  or  $02^{\circ}0$  level, both of lower energy in the  $CO_2$  molecule, the system undergoes laser action. (5-8)

The infrared  $CO_2$  laser that was used in these experiments had a laser cavity of approximately 4.25 meters and rested in an Invar frame. The water-cooled plasma of the laser was 2.25 meters long. The plasma was water-cooled because the efficiency of operation of the  $CO_2$  laser was very dependent on the temperature of the walls. Therefore, cooling with liquid nitrogen or dry ice would be expected to improve the laser efficiency. (9) A continuously flowing mixture of  $CO_2$ ,  $N_2$ , and He gases was used as the active gas in the laser at a total pressure between 8 and 13 torr, measured at the outlet of the plasma tube. The partial pressures of the gases, as well as the total pressure of the gas mixture, varied, depending on the laser line, but was typically 1-2 torr for  $CO_2$ , 1-2 torr for  $N_2$  and about 8 torr for He. The ends of the laser tube had NaCl windows mounted at the Brewster angle, requiring the laser to emit a plane-polarized light beam. One end of the laser cavity had a plane grating ruled with 150 lines per

millimeter and blazed at 10  $\mu\text{m}$ . The grating could be rotated to select different  $\text{CO}_2$  vibration-rotation transitions for laser action. At the other end of the cavity, was a partially-transmitting, dielectric-coated, germanium mirror mounted on a voltage-controlled piezoelectric translator (PZT). Either an 80% or 95% reflecting mirror could be used, depending on the strength of the laser line. The laser was stabilized on a particular laser line by a feedback loop to the PZT which varied the length of the cavity. There were two ways to monitor the fluctuations in the laser output: by monitoring the current in the plasma, or by monitoring the laser output directly. Monitoring the current was more convenient, but monitoring the laser output by means of a detector was more reliable. A model 80-214 Lansing Lock-In Stabilizer provided the DC bias voltage for the PZT. When the Model 80-214 was operated in the stabilizer mode, a 520 Hz sinusoidal voltage caused the PZT to expand and contract, which produced a 520 Hz fluctuation in the laser output unless the laser was oscillating at the top of its laser gain curve. The phase and amplitude of the fluctuations were monitored by the Lansing Stabilizer and this information was used to provide a correction signal for the DC bias to maintain the laser frequency at its value at the peak of the laser gain curve. By this means variations in laser frequency could be reduced to a few megahertz.

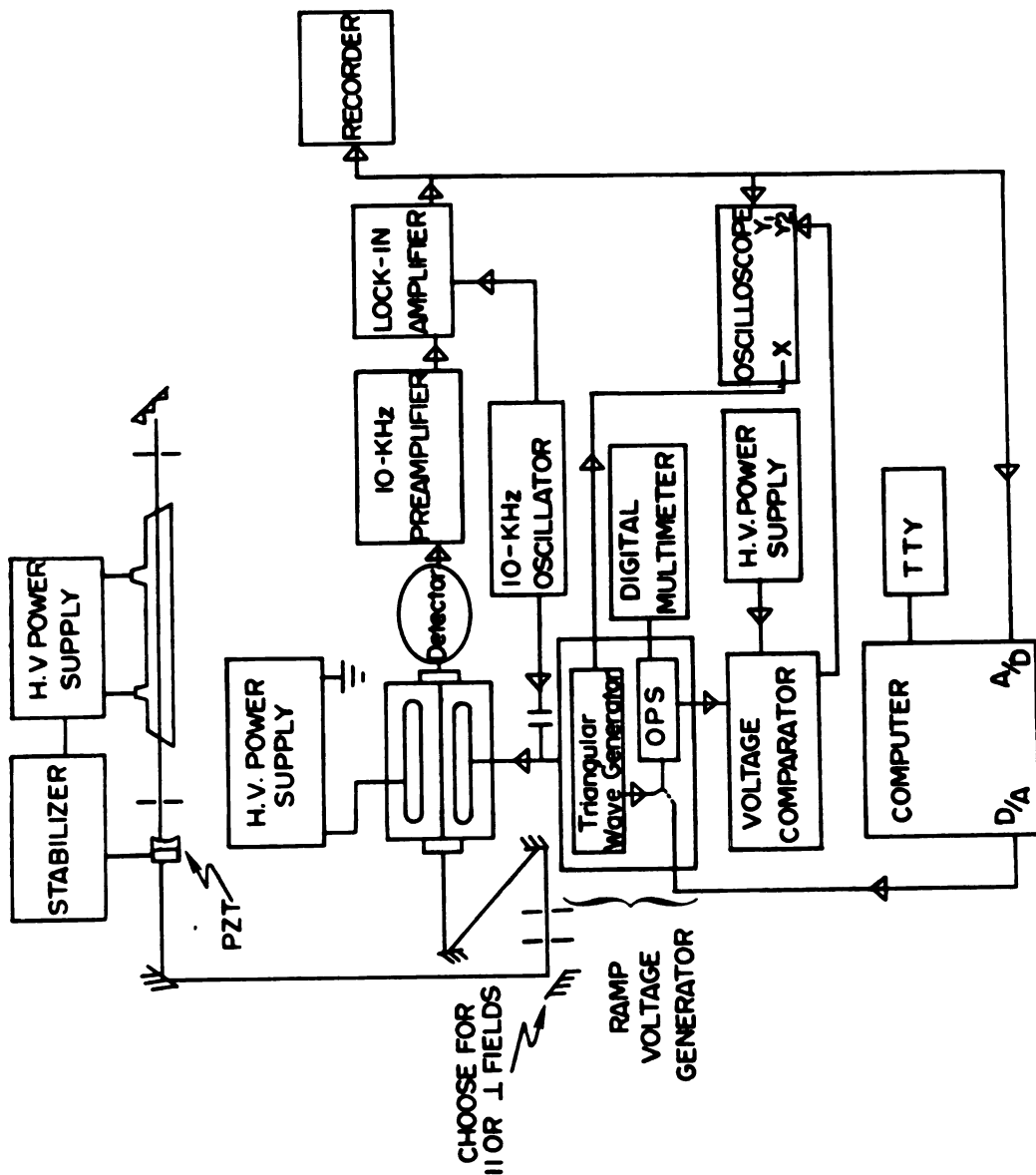
## 2.2. The Sample Cell

The sample cell for the laser Stark experiments consisted of a 15 cm diameter Pyrex pipe tee which housed two nickel plates, 40 x 5 x 2 cm, with rounded edges and broad faces that had been ground flat to within  $\pm 0.5 \mu\text{m}$ . The two nickel plates rested in a cradle and were separated by five optically polished quartz spacers which had a nominal thickness of 1 mm. To produce the desired electric field, one of the plates was connected to an operational power supply (Kepco Model 2000) and the other plate was connected to a Fluke Model 410B power supply. The sample cell was connected to a vacuum line for evacuation and sample introduction, and was fitted with a Hastings Model VT-6B vacuum gauge for rough pressure measurements. For more precise measurement, a MKS Baratron Pressure meter, type 77, was connected to the vacuum line. The sample pressure was typically 3 to 5 mtorr.

## 2.3. The Laser Stark Spectrometer

Figure 1 is a block diagram of the laser Stark spectrometer. The electric field across the sample was varied by driving the operational power supply (OPS) by the triangular wave output from a Model 112 Wavetek Signal Generator, or by stepping the OPS through its scan by the output from a digital-to-analog converter controlled by

Figure 1. A block diagram of the laser Stark spectrometer used in these experiments.



a PDP-8E computer. Voltage marker signals were produced by a zero crossover detector in a voltage comparator circuit. The OPS voltage was continuously compared to the DC voltage of a Fluke Model 412B power supply. When the voltages were equal a marker was generated. Then the electric field at the marker was calculated by adding the voltages of the two Fluke power supplies and dividing by the cell spacing. Alternately, a Keithley Model 172 Autoranging Digital Multimeter was connected to the output of the OPS so the voltage to the plates could be continuously monitored. For modulation purposes, the output of a Hewlett-Packard Model 651A audio oscillator was stepped up by an audio transformer and then mixed with the output of the OPS. A second output from the audio oscillator was used as a reference signal for a Keithley Model 840 Autoloc Amplifier for phase-sensitive detection.

By choosing the right mirror configuration, the plane polarized radiation could be sent through the sample cell with the plane of polarization either parallel or perpendicular to that of the Stark field, allowing for detection of  $\Delta M=0$  or  $\Delta M=\pm 1$  transitions. In either case, the signal was detected by a Santa Barbara Research Model 40742 Hg-Cd-Te photoconductive detector or by a Barnes Engineering Pb-Sn-Te photovoltaic detector. The 10-kHz absorption signal at the detector was proportional to the derivative of the lineshape with respect to the field because of the

small amplitude Stark modulation. The detector output was amplified by a 10-kHz tuned preamplifier, processed by the phase-sensitive detector, and sent to an oscilloscope, an analog-to-digital converter attached to the PDP-8E computer, or on occasion to a chart recorder. The data that were collected on magnetic tape by the computer were later fitted to the theoretical expression for the derivative of a Gaussian lineshape.

#### 2.4. Computer Programs

There were two main computer programs used in these experiments, BOXA and GDFITB. Program BOXA steps the output of a digital-to-analog converter from 0-10 volts, reads the output of an analog-to-digital converter after each step and records the readings on magnetic tape. Program GDFITB reads data from a magnetic tape and analyzes the data by fitting them to a theoretical lineshape.

BOXA was originally written by R. H. Schwendeman for use with a boxcar integrator, from which it takes its name. The input of BOXA includes the number of sweeps, number of channels, delay number, integration number, and timing number. The number of sweeps is the number of times the computer sweeps the Stark field from the highest to the lowest electric field. Five or ten sweeps were used in these experiments, the latter if the signal-to-noise ratio was low. The number of channels (always 200

in these experiments) is the number of steps in each sweep. The integration number was always chosen to be five and is the number of times the computer reads the analog-to-digital converter at each channel. The delay number, chosen to be five, is the number of centiseconds the computer waits after changing channels before reading the voltage. The timing number, also five, is the time in centiseconds between readings at a single channel.

The GDFITB program is a Gaussian derivative line-fitting program which is a modification by E. Bjarnov of a program originally written by R. H. Schwendeman and R. Creswell. The program reads a data file from a magnetic tape and performs a least-squares fit to the theoretical expression for the derivative of a Gaussian function. The fitting parameters of the theoretical expression are printed along with the standard deviations, variance-covariance matrix, and correlation matrix.

The reason for fitting a derivative lineshape stems from the applied experimental technique. The 10-kHz modulation that was added to the ramp voltage generator output was a relatively small amplitude AC signal which slightly varies the static electric field in the sample cell. The electric field was varied slowly enough that the molecular absorption could follow the variation without loss of coherence. When the field variation was a small fraction of the transition field width, the amplitude of the 10-kHz

oscillation at the detector was proportional to the derivative of the absorption with respect to the electric field.

The data could have been numerically integrated and fit to a Gaussian lineshape, or the derivative of the analytical equation could be calculated and the data fit directly. Because the derivative of the analytic equation for the lineshape can be taken exactly, one approximation is eliminated by the latter method and it is the preferred way.

### III. THEORY

#### 3.1. The Stark Effect

The Stark effect is the name given to the change in energy levels or spectrum of a molecule or system as a result of putting the system in an electric field.<sup>(10,11)</sup> The effect is called first order or second order Stark effect depending upon whether the change in energy is proportional to the first or second power of the electric field. If the shifts in levels are much smaller than the spacing of the levels, perturbation theory can be used to give a good approximation to the shift in energy levels. This is not the case in laser Stark spectroscopy where the level shifts are calculated by diagonalizing a Hamiltonian matrix of the form,

$$\hat{H} = \hat{H}_{\text{VR}}^{\circ} + \hat{H}_{\text{S}}. \quad (1)$$

In the dipole moment approximation the Stark portion of the Hamiltonian is  $\hat{H}_{\text{S}} = -\tilde{\mu} \cdot \tilde{\epsilon}$  where  $\mu$  is the dipole moment and  $\epsilon$  is the applied field. The matrix elements of the Hamiltonian may be computed from a basis in which the matrices of the square of the total angular momentum and the components of the angular momentum along the space-fixed Z axis and the molecule-fixed z axis are all diagonal,

$$P^2 |Jkm\rangle = \hbar^2 J(J+1) |Jkm\rangle, \quad (2)$$

$$P_z |Jkm\rangle = m\hbar |Jkm\rangle, \quad (3)$$

$$P_z |Jkm\rangle = k\hbar |Jkm\rangle. \quad (12,13) \quad (4)$$

The Hamiltonian in Equation (1) is diagonal in the quantum numbers  $k$  and  $m$ , but not in  $J$ . It turns out that the matrix for  $\hat{H}$  is of infinite dimension and therefore must be truncated at some maximum value of  $J$ . Even though  $J$  is not a good quantum number in the presence of the field, it is traditional to label the states by their zero-field  $J$  value. Thus, the wavefunction for the eigenstate  $|Jkm\rangle$  in the field is a linear combination of the wavefunctions for the states  $|Jkm\rangle$  with the same  $k$  and  $m$  values but several  $J$  values.

The nonvanishing contributions to the energy matrix are the diagonal elements, <sup>(2)</sup>

$$\begin{aligned} \langle Jkm | H_{\text{VR}}^0 | Jkm \rangle &= E_V^0 + \hbar B J(J+1) + \hbar(A-B)k^2 - \hbar D_J J^2(J+1)^2 - \\ &\quad \hbar D_{JK} k^2 J(J+1) - \hbar D_k k^4 \end{aligned} \quad (5)$$

and

$$\langle Jkm | \hat{H}_S | Jkm \rangle = \frac{-\mu \epsilon k m}{J(J+1)}, \quad (6)$$

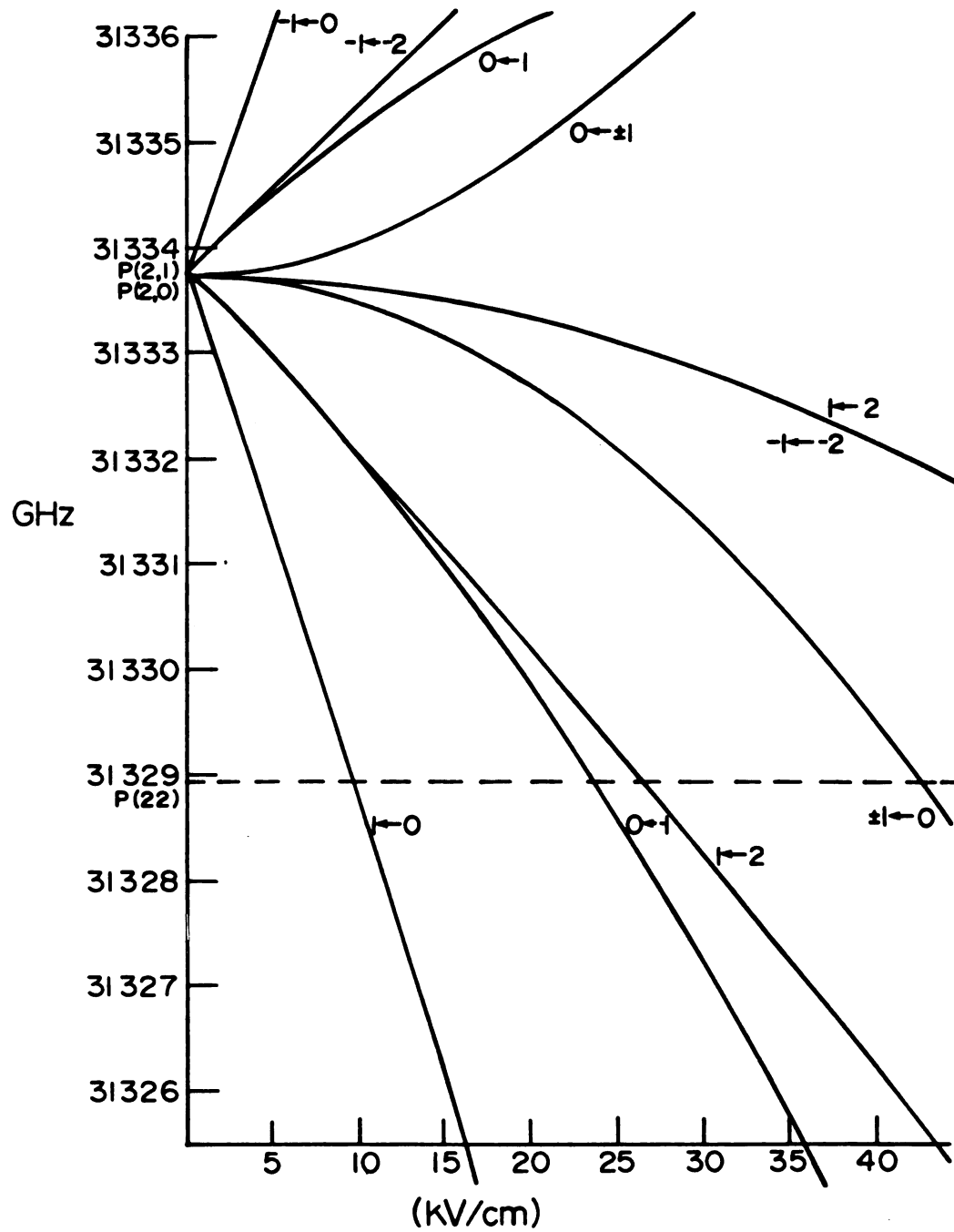
and off diagonal elements,

$$\langle J, k, m | \hat{H}_S | J \pm 1, k, m \rangle = -\mu \epsilon \left[ \frac{(J^2 - k^2)(J^2 - m^2)}{J^2(2J-1)(2J+1)} \right]^{1/2}. \quad (7)$$

In these equations, A and B are rotational constants;  $D_J$ ,  $D_{JK}$ , and  $D_K$  are centrifugal distortion constants; and  $E_v^0$  is the vibrational energy of the molecule. The eigenvalues of  $\hat{H}$  are the vibration-rotation energy levels of the molecule for a given vibrational state. The frequencies of the laser Stark spectrum are the differences in the energy for two different vibration-rotation states. Several computer programs for the calculation of laser Stark frequencies existed in our research group before this project was undertaken.

A portion of the plot of frequency as a function of electric field for methyl fluoride is shown in Figure 2. In this example, the m-components of the P(2,1) and the P(2,0) transitions are illustrated. As the electric field is increased, the m-component degeneracy is removed. Note that in this example the P(22) laser line at 31328961.530 MHz is coincident with four different sample transitions at different electric fields. The value of the laser frequency and the electric field at resonance are all that are recorded for a single line in normal laser Stark experiments, but from the lineshape the slope of the m-component can be determined and from that value the zero field frequency

Figure 2. A theoretical plot of frequency as a function of electric field for the P(2,1) and P(2,0) transitions of methyl fluoride where  $\Delta m = \pm 1$  selection rules are assumed. The dashed line represents the frequency that corresponds to the P(22) line of the CO<sub>2</sub> laser.



can be estimated.

The Stark slope may be calculated theoretically by starting with Equation (1)

$$\hat{H} = \hat{H}_{VR}^0 - \tilde{\mu} \cdot \tilde{\epsilon}, \quad (8)$$

from which it follows that

$$\partial H / \partial \epsilon = -\mu_z, \quad (9)$$

where  $\mu_z$  is the component of  $\tilde{\mu}$  in the direction of field  $\epsilon$ . Therefore, the derivative of any energy level  $W(Jkm)$  with respect to  $\epsilon$  will be given by the expectation value of  $-\mu_z$ , or

$$\left[ \frac{\partial W}{\partial \epsilon} \right]_{\epsilon = \epsilon_0} = - \langle Jkm\epsilon_0 | \mu_z | Jkm\epsilon_0 \rangle. \quad (10)$$

It is possible to calculate the expectation values from the transformation coefficients generated during the diagonalization of the Hamiltonian matrix.

### 3.2. Lineshapes

In the laboratory frame of reference the molecules in a sample cell are moving randomly in all directions, but the source of radiation is stationary. Some of the molecules have a velocity component in the direction of the radiation while others are moving toward the source. Because of their motion, the molecules see a shifted source radiation frequency. This is known as the Doppler effect, and the absorption frequency of the molecular transition is a Doppler-shifted frequency when measured in the laboratory frame of reference. If the frequency of radiation in the laboratory frame of reference is represented by  $\omega_\ell$ , then the frequency in the moving frame is

$$\omega_m = \omega_\ell \left(1 - \frac{v}{c}\right) = \omega_\ell - \omega_\ell \frac{v}{c} = \omega_\ell - \omega_s, \quad (11)$$

where  $v$  is the velocity component of the molecule in the direction of the beam,  $c$  is the velocity of the radiation, and  $\omega_s$  is the Doppler frequency shift.

The probability that a molecule will have a velocity component ( $v$ ) in the direction of the beam is given by a one-dimensional Maxwell-Boltzmann distribution,

$$p(v) = (M/2\pi k_B T)^{1/2} \exp(-Mv^2/2k_B T), \quad (12)$$

where  $M$  is the mass of the molecule,  $k_B$  is Boltzmann's

constant, and  $T$  is the absolute temperature. The probability that a molecule will have a velocity between  $v_i$  and  $v_f$  along the path of the beam is given by

$$p(v_i \rightarrow v_f) = (M/2\pi k_B T)^{1/2} \int_{v_i}^{v_f} \exp(-Mv^2/2k_B T) dv. \quad (13)$$

In the limiting case where  $v_i = -\infty$  and  $v_f = \infty$  the probability is unity.

Now consider the absorption of laser radiation by gaseous molecules. The absolute or integrated line intensities can be calculated by integrating the absorption coefficient over all frequencies.

$$\Gamma = \int_{-\infty}^{\infty} \gamma d\omega_L. \quad (14)$$

The steady state absorption coefficient for a Lorentzian lineshape at low radiation power is

$$\gamma_L(\omega_L) = \gamma_0 \frac{\Delta\omega_L^2}{(\omega_L - \omega_0 - \omega_S)^2 + \Delta\omega_L^2}. \quad (15)$$

Equation (15) may be derived from the optical Bloch equations.<sup>(14-16)</sup> The half-width at half-height for the absorption by the molecules at a single velocity is  $\Delta\omega_L$  and the peak absorption coefficient is  $\gamma_0$ , which occurs at  $\omega_L - \omega_S = \omega_0$ . The peak absorption coefficient is defined by

$$\gamma_0 = \frac{4\pi\omega_0 \mu_{if}^2 \Delta N_0}{Mc \Delta\omega_L}, \quad (16)$$

where  $\Delta N_0$  is the initial population difference between the two levels, and  $\mu_{if}$  is the transition dipole moment matrix element,

$$\mu_{if} = \langle J'k'm' | \mu_F | J''k''m'' \rangle, \quad (17)$$

where  $\mu_F$  is the molecular dipole moment along the space fixed axis F, <sup>(12)</sup> the direction of the electric vector of the applied radiation. The absorption coefficient for a large number of molecules with the velocity distribution of Equation (12) is given by

$$\gamma(\omega_\ell) = \int_{-\infty}^{\infty} p(v) \gamma_L(\omega_\ell) dv. \quad (17)$$

Since  $v = \frac{c}{\omega_\ell} \omega_s$  and  $dv = \frac{c}{\omega_\ell} d\omega_s$ , the absorption coefficient for the convolution of a Gaussian function with a Lorentzian function is <sup>(11)</sup>

$$\gamma(\omega_\ell) = (M/2\pi k_B T)^{1/2} \frac{\gamma_0 c \Delta\omega_L^2}{\omega_\ell} \int_{-\infty}^{\infty} \frac{\exp\left[-\frac{Mc^2 \omega_s^2}{2k_B T \omega_\ell^2}\right]}{(\omega_\ell - \omega_0 - \omega_s)^2 + \Delta\omega_L^2} d\omega_s. \quad (19)$$

In the Doppler limit approximation the Gaussian or exponential

term has a slowly varying contribution when compared to the Lorentzian term. Then by applying a form of the mean value theorem from calculus<sup>(18)</sup> to the Voigt profile or convolution integral, the absorption coefficient becomes

$$\gamma(\omega_\ell) = \left(\frac{M}{2\pi k_B T}\right)^{1/2} \left(\frac{4\pi\omega_o \mu^2 f \Delta N_o}{h\omega_\ell}\right) \exp\left[\frac{-Mc^2}{2k_B T\omega_\ell^2}(\omega_\ell - \omega_o)^2\right] \int_{-\infty}^{\infty} \frac{\Delta\omega_L d\omega_s}{(\omega_\ell - \omega_o - \omega_s)^2 + \Delta\omega_L^2}, \quad (20)$$

and

$$\gamma(\omega_\ell) = \left(\frac{M}{2\pi k_B T}\right)^{1/2} \left(\frac{4\pi^2\omega_o \mu^2 f \Delta N_o}{h\omega_\ell}\right) \exp\left[\frac{-Mc^2}{2k_B T\omega_\ell^2}(\omega_\ell - \omega_o)^2\right]. \quad (21)$$

The absolute or integrated line intensity can now be calculated from Equation (21),

$$\Gamma = \left(\frac{M}{2\pi k_B T}\right)^{1/2} \int_{-\infty}^{\infty} \left(\frac{4\pi^2\omega_o \mu^2 f \Delta N_o}{h\omega_\ell}\right) \exp\left[\frac{-Mc^2}{2k_B T\omega_\ell^2}(\omega_\ell - \omega_o)^2\right] d\omega_\ell, \quad (22)$$

and it follows that the integrated absorption coefficient is

$$\Gamma = \left( \frac{M}{2\pi k_B T} \right)^{1/2} \left( \frac{4\pi^2 \omega_0 \mu_{if}^2 \Delta N_0}{N} \right) \int_{-\infty}^{\infty} \frac{\exp\left[ \frac{-Mc^2}{2k_B T \omega_\ell^2} (\omega_\ell - \omega_0)^2 \right]}{\omega_\ell} d\omega_\ell. \quad (23)$$

Only the transition dipole moment  $\mu_{if}$ , the population difference  $\Delta N_0$ , and the frequency  $\omega_\ell$  will change when comparing two transitions. Therefore, the ratio of the integrated line intensities will be a ratio of the product of the square of the transition dipole moments and  $\Delta N_0$ , since the frequencies will cancel when the two transitions are on the same laser line. From Equation (21), a ratio of the absorption coefficients  $\gamma$  will yield a ratio of  $\mu_{if}^2 \Delta N_0$  if the transitions are on the same laser line also. Therefore, relative intensities can be calculated as the ratio of the absorption coefficients.

By rewriting Equation (21) as

$$\gamma(\omega_\ell) = A \exp[-q^2(\omega_\ell - \omega_0)^2], \quad (24)$$

where A is the product of several constants with the square of the transition dipole moment and  $q^2 = (Mc^2/2k_B T \omega_\ell^2)$ , the half-width at half-height of the lineshape,  $(\omega_\ell - \omega_0)_{1/2}$ , may be obtained from

$$1/2 = \exp\left[ \frac{-Mc^2}{2k_B T \omega_\ell^2} (\omega_\ell - \omega_0)_{1/2}^2 \right], \quad (25)$$

or

$$\ln 2 = \frac{Mc^2}{2k_B T \omega_\ell^2} (\omega_\ell - \omega_0)^2_{1/2} . \quad (26)$$

Therefore

$$\Delta\omega_D = (\omega_\ell - \omega_0)_{1/2} = \left( \frac{2k_B T \ln 2}{M} \right)^{1/2} \frac{\omega_\ell}{c} , \quad (27)$$

where  $\Delta\omega_D$  is called the Doppler width. The Doppler width is proportional to the frequency of the radiation and the square root of the temperature, but inversely proportional to the square root of the mass of the molecule. Then,

$$\Delta\omega_D = \omega_\ell \left( \frac{T}{M'} \right)^{1/2} (3.5815 \times 10^{-7}) , \quad (28)$$

where  $M'$  is in atomic mass units and  $T$  is the absolute temperature. (16)

The zero field frequency,  $\omega_0$  in Equation (24), may be expanded in a Taylor series in electric field and truncated after the first derivative, (19) as follows:

$$\omega_0 = \omega_0^\circ + \left( \frac{\partial \omega}{\partial \epsilon} \right)_0 (\epsilon - \epsilon_0) . \quad (29)$$

If  $\epsilon_0$  is chosen to be the field at which  $\omega_0^\circ$  equals the laser frequency  $\omega_\ell$ , then Equation (8) for the laser Stark absorption coefficient becomes,

$$\gamma(\omega_{\ell}) = A \exp \left[ -\left(\frac{\partial\omega}{\partial\epsilon}\right)_0^2 (\epsilon - \epsilon_0)^2 q^2 \right] . \quad (30)$$

The electric field is defined by

$$\epsilon = V/d , \quad (31)$$

where  $V$  is the voltage and  $d$  is the cell spacing (the distance between the two plates in the sample cell). Then if

$$q^2 \left(\frac{\partial\omega}{\partial\epsilon}\right)_0^2 / d^2 = B , \quad (32)$$

it follows that

$$\gamma(\omega_{\ell}) = A \exp \left[ -B(v - v_0)^2 \right] . \quad (33)$$

From the definition of  $q$  and Equation (32), it can be shown that the Stark slope of a transition may be estimated from the experimental value of  $B$ , as follows:

$$\left(\frac{\partial\omega}{\partial\epsilon}\right)_0 = \frac{\omega_{\ell}}{c} (2k_B T B / M)^{1/2} d . \quad (34)$$

## IV. RESULTS AND CONCLUSIONS

### 4.1. Introduction

The laser Stark spectrum of methyl fluoride was assigned and the rotation and centrifugal distortion constants determined by Freund and co-workers in 1974.<sup>(2)</sup> In their calculations of the frequency of the  $\nu_3$  band (C-F stretch) a Hamiltonian matrix truncated at  $J_{\max} = J + 5$  was used. The laser frequencies and resonant electric fields calculated by dividing their reported resonant voltages by their mean cell spacing for the transitions used in this work are given in Table I. From these known electric fields of the transitions and from the experimental resonant voltage measurements in this work, the cell spacing in the cell used here was determined by Equation (31). The transition voltage is taken as the voltage that corresponds to the maximum amplitude of the transition in the least squares fit lineshape. The transition voltage and cell spacing data are listed in Table II.

The following sections describe the results of experiments to test several questions concerning the validity of lineshape analysis in infrared laser Stark spectroscopy. The questions tested are as follows:

1. How well do the observed lineshapes match the Gaussian shape expected for Doppler-broadened spectra?

Table I. Laser Stark Transitions in  $\text{CH}_3\text{F}$  that were Studied in this Investigation.<sup>a</sup>

$\text{CO}_2$ Laser Line	Electric Field/ (V/cm)	Assignment <sup>b</sup>	$m' \leftarrow m''^c$
P(12)	21109.8	R(2,2)	1+2
"	29924.7	"	0+1
"	37991.7	R(2,1)	1+2
"	49909.7	R(2,2)	-1+0
"	57360.5	R(2,1)	0+1
P(14)	14863.6	R(1,1)	0+1
"	32680.8	"	-1+0
"	44255.8	"	2+1
"	53477.5	R(1,0)	0+±1
P(22)	9738.2	P(2,1)	1+0
"	23697.4	"	0+←-1
"	26473.5	"	1+2
"	42664.4	P(2,0)	1+0

<sup>a</sup>Data taken from S. M. Freund, G. Duxbury, M. Röhmed, J. T. Tiedje and T. Oka, J. Mol. Spec. 58, 38-57 (1974).

<sup>b</sup>R(J,k) indicates a transition from state J,k in the ground vibrational state to state J+1, k in the upper vibrational state. P(J,k) indicates a transition from state J,k to state J-1,k.

<sup>c</sup>The  $m'$  and  $m''$  are the m-quantum numbers for the upper and lower states, respectively.

Table II. Experimental Resonant Voltages Obtained from Least Squares Fits of Experimental Data to Theoretical Lineshapes and Derived Values of the Cell Spacing.

Transition <sup>a</sup>	$m' \leftarrow m$ <sup>b</sup>	V/volts <sup>c</sup>	d/cm <sup>d</sup>
R(2,2)	1+2	2172.97	0.102937
"	"	2172.42	0.102910
"	"	2172.68	0.102923
"	"	2173.85	0.102978
"	"	2173.93	0.102982
"	"	2173.78	0.102975
R(2,2)	0+1	3080.79	0.102951
"	"	3080.36	0.102937
"	"	3080.58	0.102944
"	"	3082.08	0.102995
"	"	3082.11	0.102996
"	"	3082.17	0.102998
R(2,1)	1+2	3908.35	0.102874
"	"	3907.57	0.102853
"	"	3908.16	0.102869
"	"	3909.60	0.102907
"	"	3909.67	0.102909
"	"	3909.85	0.102913
R(2,2)	-1+0	5139.46	0.102975
"	"	5139.85	0.102983
"	"	5139.83	0.102983
"	"	5141.22	0.103010
"	"	5141.48	0.103016
"	"	5141.49	0.103016
R(2,1)	0+1	5904.35	0.102934
"	"	5904.81	0.102942
"	"	5905.05	0.102946
"	"	5907.35	0.102986
"	"	5907.38	0.102987
"	"	5907.19	0.102984
R(1,1)	0+1	1528.60	0.102842
"	"	1528.58	0.102840
"	"	1528.57	0.102840

Table II. Continued.

Transition <sup>a</sup>	$m' \leftarrow m$ <sup>b</sup>	V/volts <sup>c</sup>	d/cm <sup>d</sup>
R(1,1)	-1 $\leftarrow$ 0	3364.46	0.102949
"	"	3364.52	0.102951
"	"	3364.79	0.102959
R(1,1)	2 $\leftarrow$ 1	4556.30	0.102954
"	"	4558.46	0.102303
"	"	4557.94	0.102991
R(1,0)	0 $\leftarrow$ $\pm$ 1	5505.43	0.102949
"	"	5504.42	0.102930
"	"	5505.39	0.102948

<sup>a</sup>See footnote b, Table I.

<sup>b</sup>See footnote c, Table I.

<sup>c</sup>Resonant voltage obtained from a least squares fit of the lineshape to a derivative of a Gaussian function.

<sup>d</sup>The cell spacings (d) are obtained by combining the resonant voltages in this table with the resonant voltages and mean cell spacing in Reference (2). The mean cell spacing,  $\bar{d}=0.102947\pm 0.000097$  cm, where the uncertainty is two standard deviations.

2. What is the effect of changing sample pressure on the observed lineshape?
3. Are the transitions broadened by either the modulation of the laser used for laser frequency stabilization or by the modulation of the electric field used for observation of the spectra?
4. Can the linewidths obtained be used with the expected Doppler width to determine the derivative of the frequency of the transition with respect to the electric fields?
5. Do the amplitudes of the transitions obtained from the fits of the lineshapes for several transitions observed with a single laser line vary according to the theoretical intensities of the transitions?
6. Are the amplitudes of a single transition obtained from fits of lineshapes at several pressures proportional to the sample pressure?

In the remaining sections of this chapter the results of the examination of these questions will be discussed.

#### 4.2. The Gaussian Lineshape

An important question to be answered before any results are presented or conclusions drawn is how well the data fit the derivative Gaussian lineshape. The fact that it is a derivative lineshape is an artifact of the applied

experimental technique (Section 2.4). The equation that is fit is the voltage derivative of a form of Equation (33) to which empirical slope (D) and base line (E) terms have been added, as follows:

$$F(V) = A(V-C)\exp[-B(V-C)^2] + D(V-C) + E. \quad (35)$$

An oscilloscope plot of a data set for the R(1,1)  $m=-1 \rightarrow 0$  transition is shown in the photograph of Figure (3) and a corresponding plot of the difference between the observed and calculated values is shown in the photograph of Figure (4). The scatter in Figure (4) shows a random pattern and therefore indicates that there are no obvious systematic deviations from the Gaussian lineshape. The fact that the standard deviations of the observed minus calculated data points is only 0.1-2.0% of the difference between the maximum and the minimum relative intensity values is also an indication that the data fit the Gaussian lineshape quite well.

#### 4.3. Modulation Broadening

In the laser Stark spectrometer there are two possible sources of modulation broadening: one from the laser frequency modulation that is used to stabilize the laser, and the second from the 10 kHz voltage that is added to the Stark field to modulate the absorption. Both are important

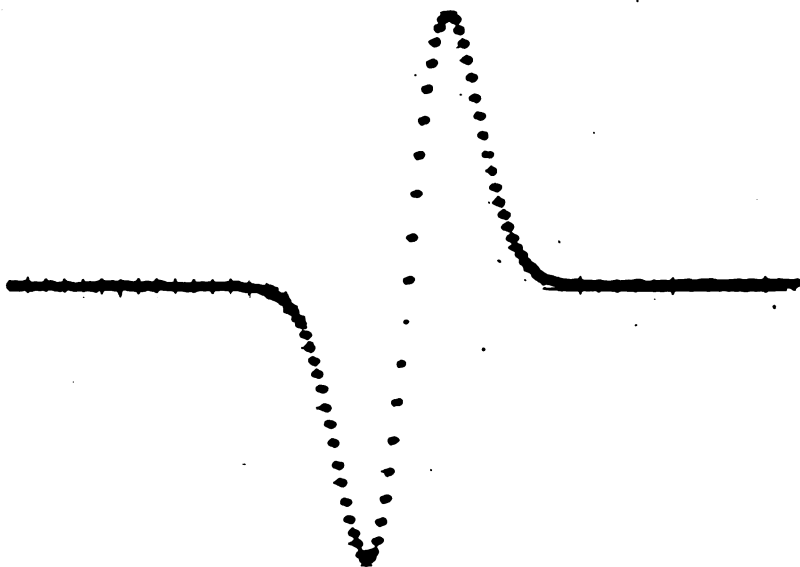


Figure 3. A photograph of an oscilloscope plot of a data file for the R(1,1)  $m=-1+0$  transition in methyl fluoride.



Figure 4. A photograph of an oscilloscope plot of the difference between an experimentally observed data set and the best theoretical Gaussian lineshape for the  $R(1,1)_{m=-1+0}$  transition in methyl fluoride magnified 140 times.

points of concern and will be discussed here.

The purpose of modulating the laser frequency is to keep the laser functioning at the frequency that is at the peak of the laser gain curve. A laser gain curve is a graph of power output as a function of frequency or wavelength. If the modulation amplitude becomes too large, the monochromaticity of the laser is lost. For example, a modulation voltage of 13.9 volts peak-to-peak applied to the piezoelectric translator used in this investigation results in a 1 MHz frequency variation. This is similar to the effect of opening the slits in a conventional monochromator. In Tables III and IV the measured Doppler width and the laser frequency modulation voltage are listed for several data sets for the  $R(1,1)$ ,  $m=0+1$ , and the  $R(1,0)$ ,  $m=0+1$ , transitions. The Doppler width appears to increase with increasing modulation voltage, but for the various modulation amplitudes shown the increase is not much larger than the random error. To reduce the broadening from this effect the modulation voltage was kept as low as possible (5-48 volts peak-to-peak) consistent with maintaining stabilization of the laser.

The 10 kHz modulation signal that is added to the Stark field is the second source of modulation broadening. The modulation amplitude for the Stark slope and relative intensity experiments described in Sections 4.5 and 4.6 was either 4.1 or 4.6 volts, peak-to-peak. This small

Table III. Variation of the Apparent Doppler Width of the R(1,1), m=0+1 Transition with the Voltage Applied to the Piezoelectric Translator.

Voltage/volts <sup>a</sup>	B/(volts) <sup>-2b</sup>	$\Delta\nu_D$ /MHz <sup>c</sup>
10	0.009171(30) <sup>d</sup>	43.59(9) <sup>d</sup>
20	0.009488(27)	42.86(8)
30	0.009556(29)	42.71(8)
40	0.009514(28)	42.80(8)
50	0.009500(27)	42.83(8)
60	0.009553(26)	42.71(8)
90	0.009422(30)	43.01(9)
100	0.009464(27)	42.91(8)

<sup>a</sup>Peak-to-peak amplitude of the sinusoidal voltage applied to the PZT.

<sup>b</sup>Exponential parameter in the fit of the lineshape (Equation (35)).

<sup>c</sup> $\Delta\nu_D = [dv/d\epsilon]/d \left(\frac{\ln 2}{B}\right)^{1/2}$  from Equations (26) and (32) and the definition of q.

<sup>d</sup>The standard deviation in the last digit quoted is in parentheses.

Table IV. Variation of the Apparent Doppler Width of the R(1,0),  $m=0\pm 1$  Transition with the Voltage Applied to the Piezoelectric Translator.

Voltage/volts <sup>a</sup>	$B/(\text{volts})^{-2}$ <sup>b</sup>	$\Delta v_D/\text{MHz}$ <sup>c</sup>
10	0.003491(4) <sup>d</sup>	36.50(4) <sup>e</sup>
20	0.003513(4)	36.38(4)
30	0.003491(3)	36.49(3)
40	0.003493(3)	36.49(3)
50	0.003494(3)	36.50(3)
60	0.003486(4)	36.52(4)
70	0.003482(4)	36.54(4)
80	0.003505(3)	36.42(3)
100	0.003473(3)	36.59(3)

<sup>a</sup>See footnote a, Table III.

<sup>b</sup>See footnote b, Table III. The values for B are the averages of from 3 to 5 values.

<sup>c</sup>See footnote c, Table III.

<sup>d</sup>See footnote d, Table III. The standard deviations were

calculated by using the equation,  $\sigma_{\text{ave}} = \left( \sum_{i=1}^n \frac{\sigma_i^2}{n} \right)^{1/2}$ .

<sup>e</sup>See footnote d, Table III.

voltage may be as much as 0.5% of the Stark field, as in the case of the P(2,1),  $m=1+0$  transition. More recently, experiments were performed at slightly higher pressures and smaller amplitude modulation voltages (1.4 and 0.73 volts peak-to-peak). Slightly narrower lines ( $\delta\Delta\nu_D \approx 0.3$  MHz) resulted from this decrease in modulation voltage (see Table VI). Up to a point, higher modulation voltages are favored, because they lead to larger signals and greater signal-to-noise ratio. However, from these results it is apparent that the smallest possible modulation voltage should be used if accurate line-width information is desired.

#### 4.4. The Effect of Sample Pressure

As the pressure of the sample is increased, the line-shape should change and become pressure broadened. As the pressure increases, the molecules experience more collisions per unit time, and collision-broadening is the dominant mode of pressure-dependent broadening. The pressure broadening parameters of the transitions studied in this work are not known, but rotational linewidths in  $\text{CH}_3\text{F}$  are of the order of 17 MHz/torr.<sup>(20)</sup>

Tables V and VI show the relationship between  $\Delta\nu_D$  and pressure. Presumably at higher pressures  $\Delta\nu_D$  will increase, but since the experiments were performed at such low pressures, pressure broadening should be

Table V. The Effect of Moderate Pressure Changes on the Apparent Doppler Width for the R(1,1),  $m=0+1$  Transition.

Pressure/mtorr <sup>a</sup>	$B/(\text{volts})^{-2}$ <sup>b</sup>	$\Delta\nu_D/\text{MHz}$ <sup>c</sup>
3.47	0.014062(73) <sup>d</sup>	35.21(11) <sup>d</sup>
3.49	0.014136(62)	35.11(9)
3.52	0.014033(48)	35.24(8)
3.54	0.014370(14)	34.83(3)
3.58	0.014372(13)	34.82(3)
9.52	0.014943(10)	34.15(3)
9.51	0.014971(9)	34.12(3)
9.51	0.015052(12)	34.02(3)
9.51	0.015007(15)	34.08(3)
11.23	0.015210(14)	33.85(3)
11.30	0.015094(11)	33.98(3)
11.38	0.015180(10)	33.88(3)
11.45	0.015054(10)	34.03(3)

<sup>a</sup>Pressure in mtorr, as measured with the MKS Baratron Gauge.

<sup>b</sup>See Table III, footnote b.

<sup>c</sup>See Table III, footnote c.

<sup>d</sup>See Table III, footnote d.

Table VI. The Effect of Moderate Pressure Variations on the Apparent Doppler Width of the P(2,1),  $m=1\leftarrow 0$  Transition.

Pressure/ mtorr <sup>a</sup>	Stark Modulation/ Volts	$B/(\text{volts})^{-2}$ <sup>b</sup>	$\Delta\nu_D/\text{MHz}$ <sup>d</sup>
50.45	0.73	0.015221(49) <sup>e</sup>	33.80(7) <sup>f</sup>
44.77	0.73	0.015383(36)	33.62(6)
36.56	0.73	0.015233(60)	33.78(8)
30.76	0.73	0.015231(43)	33.79(5)
27.30	0.73	0.015333(42)	33.67(6)
22.81	0.73	0.015267(43)	33.75(6)
19.81	0.73	0.015378(42)	33.62(6)
19.92	1.4	0.015192(31)	33.83(5)
16.77	1.4	0.015404(59)	33.59(8)
12.92	1.4	0.015505(38)	33.49(6)
10.13	1.4	0.015349(35)	33.65(5)
6.80	1.4	0.014990(36)	34.06(6)
3.00	1.4	0.015010(48)	34.03(7)

<sup>a</sup>See footnote a, Table V. The values reported are the average of three trials.

<sup>b</sup>The peak-to-peak modulation voltage applied to the Stark cell for signal detection.

<sup>c</sup>See footnote b, Table III. The values are the average of three trials.

<sup>d</sup>See footnote c, Table III.

<sup>e</sup>See footnote d, Table IV.

<sup>f</sup>See footnote d, Table III.

insignificant. The pressure of the gas sample was kept between two and five millitorr for the laser Stark slope and relative intensity experiments. The pressure was kept low to avoid electric discharge in the sample cell at high electric fields.

From the tables it appears that a pressure of 10-13 millitorr would have been a better pressure to conduct relative intensity and Stark slope experiments, since there appears to be a narrower Doppler width in this pressure range. This may be explained by considering the signal-to-noise ratio and the laser stability. The signal-to-noise ratio should be higher at moderately higher pressure. Therefore, if the scatter were signal-to-noise dependent, the scatter would be less at moderately higher pressures. It appears that the scatter is independent of the sample pressure; therefore, the scatter is probably a result of fluctuations in the laser output.

#### 4.5. Determination of the Laser Stark Slopes

The half-width at half-maximum of the laser Stark lineshape was investigated in order to determine whether the slope of a laser Stark transition (derivative of the frequency with respect to the Stark electric field) could be resolved from a study of lineshapes. In Chapter III the effective electric field width ( $B^{-1/2}$ ) of a laser Stark transition is predicted to be a function of the

Doppler width and Stark slope (Equations (32) and (27) and the definition of  $q$ ). The Doppler width depends only on the mass of the molecule, the frequency of the transition, and the temperature. Therefore, it is possible to calculate it for a given transition in a given molecule.

According to Equations (27) and (32) and the definition of  $q$ ,  $B^{1/2}$  is proportional to  $(dv/d\epsilon)(\ln 2)^{1/2}/d$ . Therefore, from a plot of  $B^{1/2}$  as a function of the scaled Stark slope, the Doppler width can be determined as the reciprocal of the slope (Figure 5). The predicted Doppler width at 24°C for  $\text{CH}_3\text{F}$  is 33.39 MHz and the experimental value of 34.54 MHz is only 3.4% wider than the theoretical value.

From the theoretical value for the Doppler width, calculated values for the laser Stark slopes have been determined and are listed in Table VII. All of the entries in Table VII show a smaller absolute slope than their corresponding theoretical values (from 0.17 to 19 kHz per unit electric field (volts/cm) smaller). If the effective electric field linewidth is larger than it should be because of some broadening process, then the effective exponential parameter  $B$  will be smaller than it should be. This wider effective electric field width is then the cause of the smaller absolute slope. Nevertheless, it is clear that for  $\text{CH}_3\text{F}$ , at least, the measured linewidths could have been used to predict the Stark slope of the

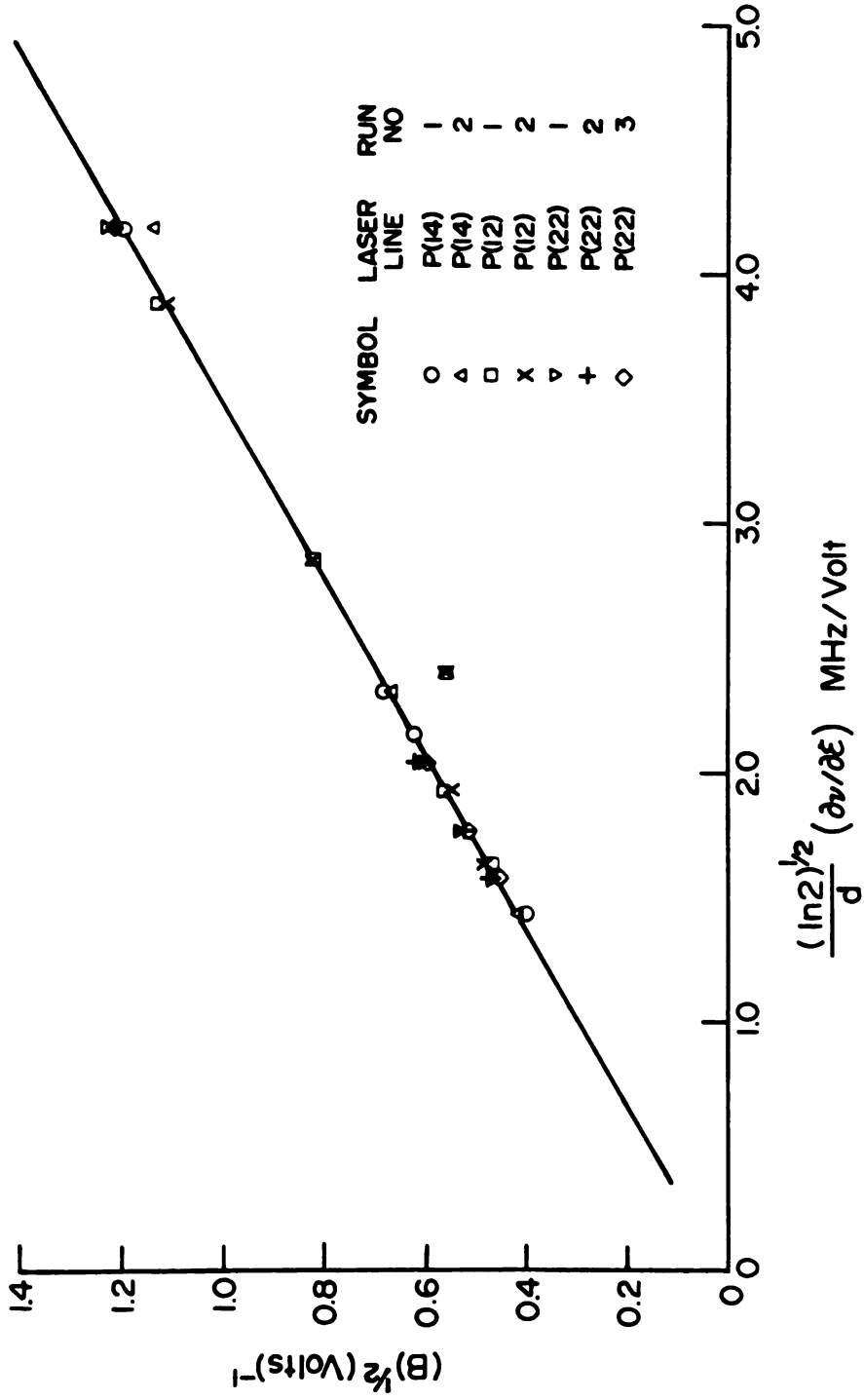


Figure 5. A graph of the square root of the exponential parameter as a function of the scaled Stark slope for determination of the Doppler width.

Table VII. Laser Stark Slopes Determined from Experimental Data for the Transitions Investigated.

Transition <sup>a</sup>	$m'+m''^b$	$\frac{B^{1/2}}{(\text{volts})^{-1}}$	$(\frac{d\nu}{d\epsilon})$ Exp. <sup>c</sup>	$(\frac{d\nu}{d\epsilon})$ Theory <sup>d</sup>
R(1,1)	0+1	0.1205	0.4970	0.516222(0.019) <sup>e</sup>
R(1,1)	-1+0	0.0685	0.2825	0.287156(0.0047)
"		0.0674	0.2780	" (0.0092)
R(1,1)	2+1	0.0403	0.1662	0.177035(0.011)
"		0.0419	0.1728	" (0.0042)
R(1,0)	0+±1	0.0628	0.2590	0.266647(0.0076)
R(2,2)	1+2	0.1130	0.4668	0.478959(0.012)
"		0.1121	0.4631	" (0.016)
R(2,2)	0+1	0.0828	0.3421	0.352071(0.010)
"		0.0828	0.3421	" (0.010)
R(2,2)	-1+0	0.0563	0.2326	0.237892(0.0053)
"		0.0553	0.2285	" (0.0094)
R(2,1)	0+1	0.0472	0.1950	0.202120(0.0071)
"		0.0478	0.1975	" (0.0046)
P(2,1)	1+0	0.1230	-0.5038	-0.515571(-0.012)
"		0.1217	-0.4985	" (-0.017)
"		0.1222	-0.5006	" (-0.015)
P(2,1)	0+--1	0.0611	-0.2503	-0.250673(-0.00037)
"		0.0612	-0.2505	" (-0.00017)
"		0.0606	-0.2482	" (-0.0025)
P(2,1)	1+2	0.0465	-0.1905	-0.194744(-0.0042)
"		0.0470	-0.1925	" (-0.0022)
"		0.0466	-0.1909	" (-0.0038)
P(2,0)	±1+0	0.0529	-0.2167	-0.217445(-0.00075)
"		0.0527	-0.2159	" (-0.0015)
"		0.0526	-0.2155	" (-0.0019)

Table VII. Continued.

<sup>a</sup>See Table I, footnote b.

<sup>b</sup>See Table I, footnote c.

<sup>c</sup>The units are MHz/(volt/cm) and the values were calculated by Equation (34).

<sup>d</sup>The units are MHz/(volt/cm). The values were determined by the computer program LSINT.

<sup>e</sup>The values in parenthesis are  $(dv/d\varepsilon)$  Theory- $(dv/d\varepsilon)$  exp.

transitions to within a few percent. An apparent exception, for which we have no explanation at present, is the  $R(2,1)$ ,  $m=1+2$ , transition.

#### 4.6. Relative Intensities

Figure (6) represents the relationship between theoretical intensities and the pre-exponential ( $A$  in Equation (24)) from fitted data, while Figure (7) shows the correlation between theoretical intensities and the calculated relative areas of the absorption curves. The relative areas have been calculated by multiplying each amplitude by the corresponding full width at half maximum. All of the lines on both graphs have been fit to a linear equation whose parameters can be found in Table VIII. From a comparison of the correlation coefficients Figure (6) shows a better relationship between predicted and experimental intensities than does Figure (7); i.e., the data are more highly correlated to a straight line when the amplitude instead of the area is compared. However, differences in correlation coefficients may not be real, as they are very small. Nevertheless, there appears to be no reason to go through the extra trouble of calculating areas.

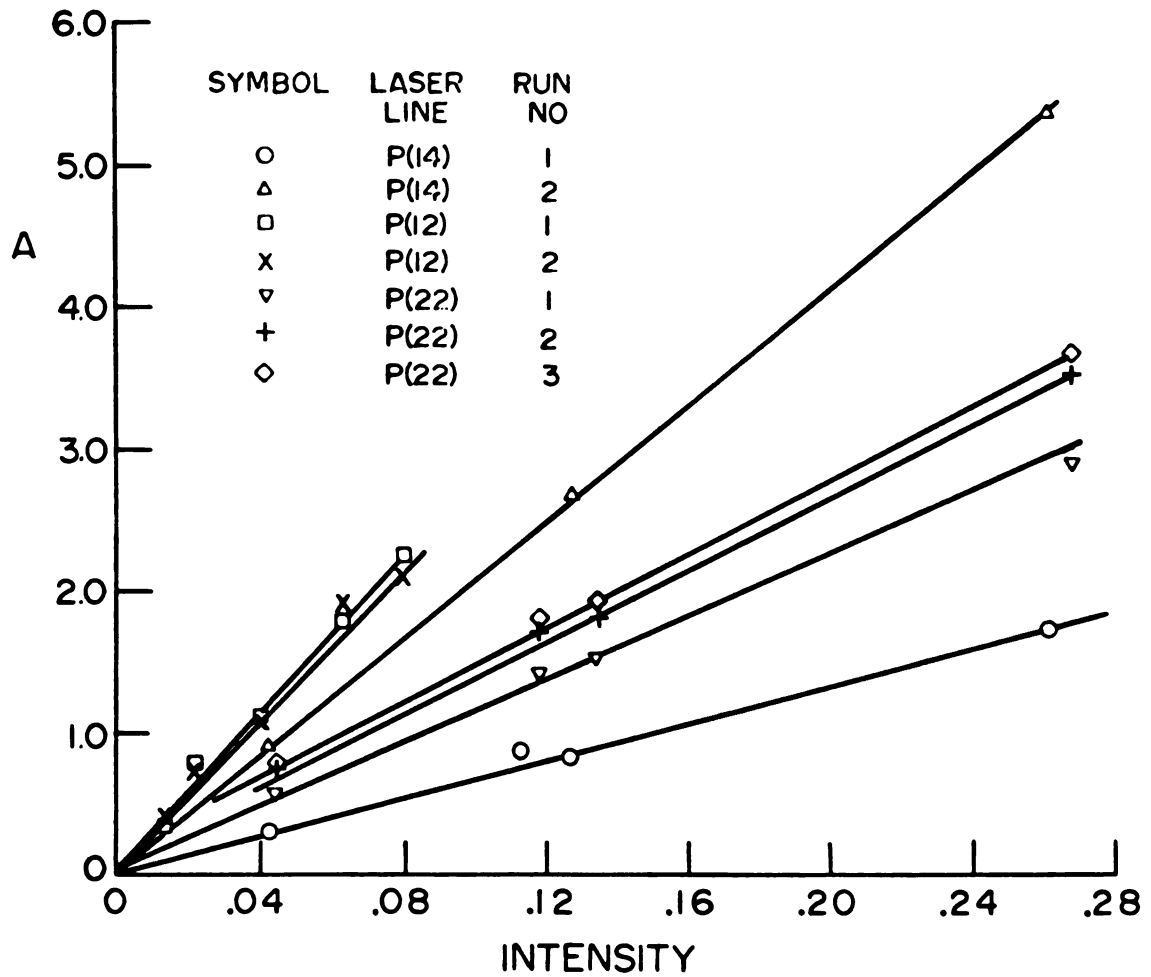


Figure 6. A graph of the signal (pre-exponential) as a function of theoretical intensity.

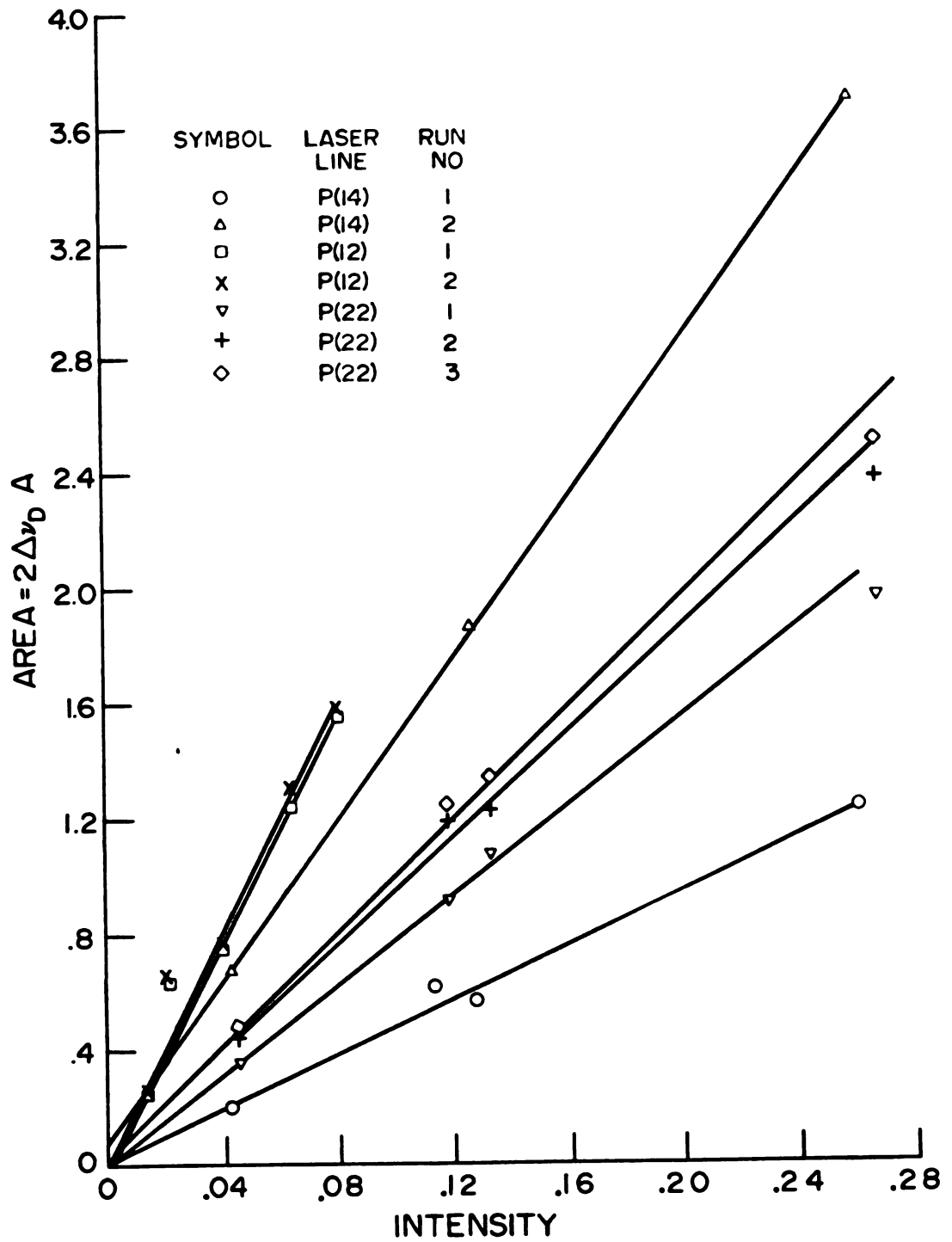


Figure 7. A graph of the area of a transition as a function of the theoretical intensity.

Table VIII. Linear Least Squares Parameters for the Relative Intensity Data Depicted Graphically in Figures (6) and (7).

Laser Line	Fig.	Run No.	Slope	Intercept	Correlation Coefficient
P(14)	6	1	0.1536	-0.00774	0.993
"	"	2	0.0491	-0.00367	1.000
P(12)	"	1	0.0362	-0.00131	0.995
"	"	2	0.0375	-0.00303	0.990
P(22)	"	1	0.0950	-0.0109	0.997
"	"	2	0.0785	-0.0106	0.999
"	"	3	0.0750	-0.0112	0.999
P(14)	7	1	0.1777	-0.00382	0.994
"	"	2	0.0600	-0.00736	1.000
P(12)	"	1	0.0444	-0.00335	0.981
"	"	2	0.0457	-0.00514	0.979
P(22)	"	1	0.1150	-0.00746	0.996
"	"	2	0.0970	-0.0121	0.998
"	"	3	0.0916	-0.0119	0.998

#### 4.7. The Dependence of Absorption on Sample Pressure

The Beer-Lambert-Bouguer law relates the path length of the radiation, the molar absorptivity, and the concentration to the absorption. The molar absorptivity and path length are constants for a given gas, transition, and absorption cell. According to the ideal gas law the concentration of a gaseous sample is proportional to its partial pressure. Therefore, there should be a linear relationship between the pre-exponential in the fitting equation (Equation (24)) and the pressure. Some typical results of pressure dependence of the pre-exponentials at three different levels of modulation amplitude are shown in Figure (8). The large fluctuation between points is believed to be due to the variation in the absolute power output of the laser. However, the mean intensities at the various pressures (also plotted) follow the straight lines rather well.

#### 4.8. Discussion

There are at least three applications of the results of this study: gas mixture analysis, laser Stark slope estimation, and measurement of pressure broadening parameters. In the analysis of gas mixtures, intensity appears to be a linear function of pressure for a given laser line with a mean deviation of average measurements of

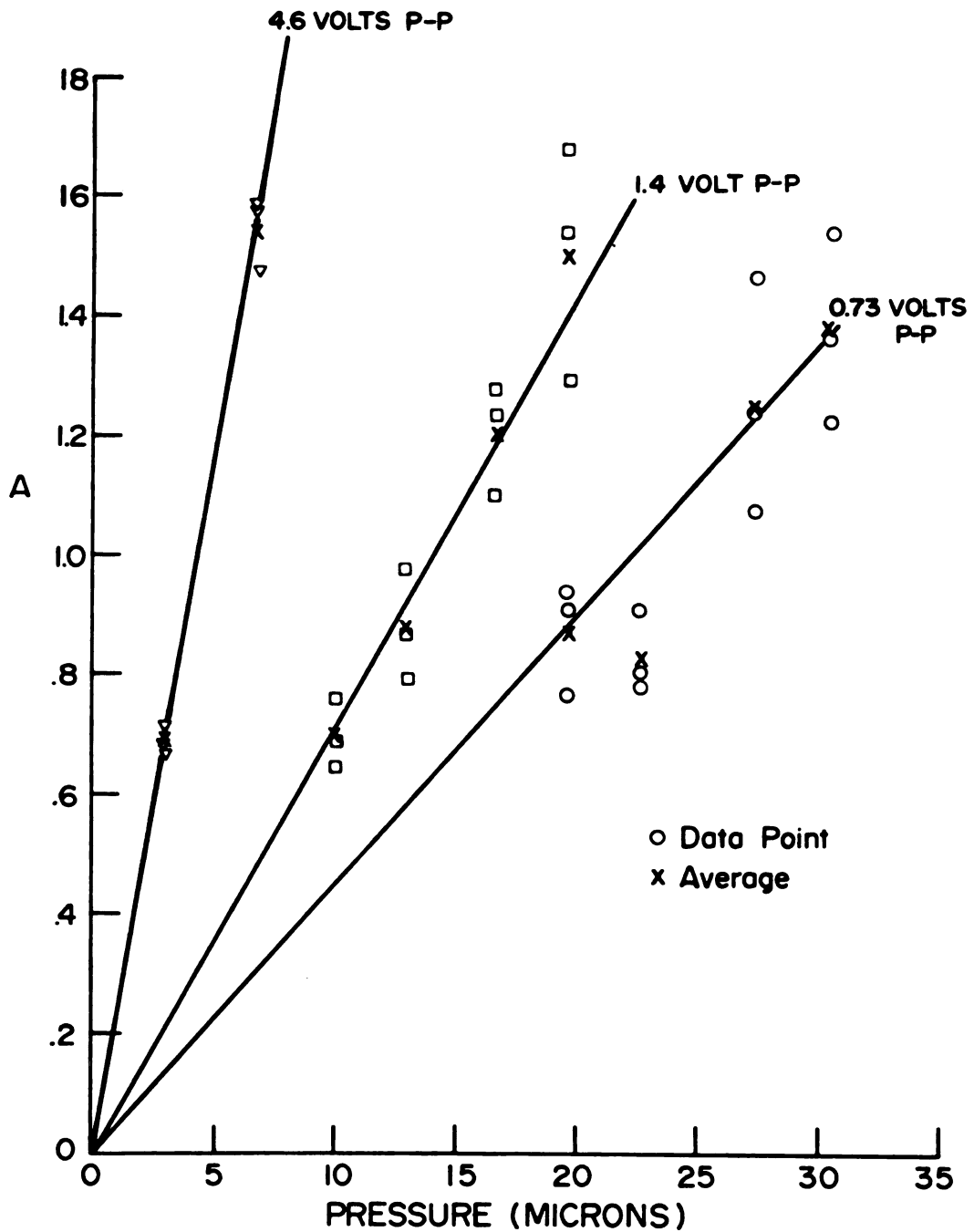


Figure 8. A graph of relative intensity as a function of pressure for the  $P(2,1)$   $m=1+0$  transition at three different Stark modulation amplitudes.

4.7%. Relative intensities of transitions occurring at different fields with the same laser line follow predicted values to about 5.3%. In the transitions studied here, where the laser Stark slopes were estimated from line widths, the deviation from predicted values were about 2.3%. Thus laser Stark slope estimation should prove very useful in assignment of laser Stark transitions and the next step would be an application to such assignment. The third application is the measurement of pressure broadening by the study of lineshapes at higher pressures. In order to obtain significant pressure broadening, pressures will have to be of the order of one torr or larger, and consequently resonant fields must be low. This will require either near coincidence of laser frequency and zero field absorption frequency or a tunable laser.

There are several improvements to be made and future experiments to be carried out. In terms of experimental improvements, a better method of laser frequency stabilization and some method for compensation for fluctuation of laser power are needed. For the latter, the relative laser power output for each recorded data point could be measured, and the ratio of the spectral intensity to relative power stored. This would be analogous to a double beam spectrophotometer. There are two additional experiments that should be performed; a different molecule with a different molecular weight should be studied

and a series of experiments should be carried out at temperatures other than room temperature. The only parameters that were not changed in the Doppler width equation during any of these experiments were mass and temperature. Studying the mass variation should be simpler than the temperature variation because of the difficulty in keeping such a large sample cell at some constant temperature different from room temperature.

## REFERENCES

## REFERENCES

1. K. Sakurai, K. Uehara, M. Takami, and K. Shimoda, *J. Phys. Soc. Japan* 23, 103 (1967).
2. S. M. Freund, G. Duxbury, M. Römheld, J. T. Tiedje, and T. Oka, *J. Mol. Spectrosc.* 52, 38-57 (1974).
3. Chikashi Yamada and Eizi Hirota, *J. Mol. Spectrosc.* 64, 31-46 (1977).
4. T. Amano and R. H. Schwendeman, *J. Chem. Phys.* 68, 530-537 (1978).
5. Arnold Bloom, *Gas Lasers*, John Wiley & Sons, Inc., New York 1968.
6. L. Allen and D. G. C. Jones, *Principles of Gas Lasers*, Plenum Press, New York, 1967.
7. C. K. N. Patel, *Phys. Rev. Lett.* 13, 617-619 (1964).
8. Donald O'Shea, William T. Rhodes, and W. Russell Callen, *A Laser Textbook. An Introduction to Lasers and Their Applications*, Lecture Notes, Georgia Institute of Technology, Atlanta, 1975.
9. Reference 5, p. 10-11.
10. C. H. Townes and A. L. Schawlow, *Microwave Spectroscopy*, Dover Publishing, Inc., New York, Chapter 10, 1975.
11. W. Gordy and R. L. Cook, *Microwave Molecular Spectra*, Interscience Publishers, New York, Chapter 10, 1970.
12. M. W. P. Strandberg, *Microwave Spectroscopy*, John Wiley & Sons, Inc., New York, Chapter 1, 1954.
13. R. H. Schwendeman, *J. Mol. Spectrosc.* 7, 280-286 (1961).
14. J. I. Steinfeld, *Molecules and Radiation*, Harper & Row, New York, Chapter 12, 1974.
15. W. H. Flygare, *Molecular Structure and Dynamics*, Prentice-Hall Inc., Englewood Cliffs, New Jersey, 448-455, 1978.
16. R. H. Schwendeman, unpublished.

17. Reference 15, p. 432-436.
18. Taylor and Mann, Advanced Calculus, 2nd Ed., Xerox, Lexington, Massachusetts, 113, 1972.
19. R. H. Schwendeman, personal communication.
20. G. Birnbaum, E. R. Cohen, and J. R. Rusk, J. Chem. Phys. 49, 5150-5156 (1968).

MICHIGAN STATE UNIV. LIBRARIES



31293009989348